Process Biochemistry 49 (2014) 409–417

Contents lists available at ScienceDirect

Process Biochemistry

journal homepage: www.elsevier.com/locate/procbio

A novel enantioselective epoxide hydrolase from *Agromyces mediolanus* ZJB120203: Cloning, characterization and application

Feng Xue[a,b], Zhi-Qiang Liu[a,b], Shu-Ping Zou[a,b], Nan-Wei Wan[a,b], Wen-Yuan Zhu[a,b], Qing Zhu[a,b], Yu-Guo Zheng[a,b,*]

[a] *Institute of Bioengineering, Zhejiang University of Technology, Hangzhou 310014, Zhejiang, PR China*
[b] *Engineering Research Center of Bioconversion and Biopurification of the Ministry of Education, Zhejiang University of Technology, Hangzhou 310014, Zhejiang, PR China*

ARTICLE INFO

Article history:
Received 31 October 2013
Received in revised form
24 December 2013
Accepted 7 January 2014
Available online 18 January 2014

Keywords:
Cloning
Characterization
Epoxide hydrolase
Agromyces mediolanus ZJB120203
(*S*)-Epichlorohydrin

ABSTRACT

A new strain *Agromyces mediolanus* ZJB120203, capable of enantioselective epoxide hydrolase (EH) activity was isolated employing a newly established colorimetric screening and chiral GC analysis method. The partial nucleotide sequence of an epoxide hydrolase (AmEH) gene from *A. mediolanus* ZJB120203 was obtained by PCR using degenerate primers designed based on the conserved domains of EHs. Subsequently, an open reading frame containing 1167 bp and encoding 388 amino acids polypeptide were identified. Expression of AmEH was carried out in *Escherichia coli* and purification was performed by Nickel-affinity chromatography. The purified AmEH had a molecular weight of 43 kDa and showed its optimum pH and temperature at 8.0 and 35 °C, respectively. Moreover, this AmEH showed broad substrates specificity toward epoxides. In this study, it is demonstrated that the AmEH could unusually catalyze the hydrolysis of (*R*)-ECH to produce enantiopure (*S*)-ECH. Enantiopure (*S*)-ECH could be obtained with enantiomeric excess (*ee*) of >99% and yield of 21.5% from 64 mM (*R,S*)-ECH. It is indicated that AmEH from *A. mediolanus* is an attractive biocatalyst for the efficient preparation of optically active ECH.

1. Introduction

Epoxide hydrolases (EHs, EC 3.3.2.3), ubiquitous in nature and co-factor independent enzymes, catalyze the hydrolysis of epoxides to corresponding vicinal diols with the addition of a water molecule [1,2]. EHs have been isolated or cloned from a wide range of organisms including bacteria, yeast, fungi, plant, insect, and mammals [3–8]. Most EHs are members of the α/β hydrolase fold family base on their available sequences information [9–11]. These EHs consist of a core domain that is composed of a central β-sheet surrounded by α-helices and a variable cap domain positioned on top of the substrate binding site. They use a catalytic mechanism that involves an Asp–His–Asp/Glu (nucleophile–histidine-acid) catalytic triad located on top loops of the main domain [12].

The observed intrinsic enantioselectivity of some EHs makes them more useful in the preparation of enantiopure pharmaceuticals and fine chemicals [11–15]. In particular, enantiopure epichlorohydrin (ECH) is a valuable intermediate for producing optically active pharmaceuticals such as β-blockers, L-carnitine, and ferroelectric liquid crystals [16]. To develop the needs of high performance enzymes, recent efforts have been focused on the searching, cloning, expression, purification, characterization, catalytic mechanism, modification of enantioselectivity and activity, resolution of structure and homology modeling of various new EHs. Some of EHs exhibit modest enantioseletivities toward ECH. However, only a few could preferentially hydrolyze (*R*)-ECH, retaining the useful (*S*)-ECH for the synthesis of atorvastatin. For example, *Novosphingobium aromaticivorans* EH has been cloned and applied into resolution of (*R,S*)-ECH (50 mM) to provide (*S*)-ECH with 20.7% yield and more than 99% enantiomeric excess (*ee*) [16]. Enantiopure (*S*)-ECH could be obtained from its racemates (60 mM) with an optical purity of 100% *ee* and 20% yield in cyclohexane supplemented with 2.0% (v/v) water using *Aspergillus niger* cells harboring EH [17]. 18.5% of (*S*)-ECH with 98% *ee* from racemic ECH was obtained by the dry cells of *A. niger* ZJB-09173 in cyclohexane supplemented with 4.0% (v/v) water [18]. Hence, exploring new enantioselective EHs is necessary due to the limited number of EHs for the enantioselective production of (*S*)-ECH.

In this study, a new strain, *Agromyces mediolanus* ZJB120203 producing a novel EH was isolated and identified. The gene encoding the EH from *A. mediolanus* ZJB120203 was cloned and expressed in *Escherichia coli*. Some characteristics of recombinant EH as well as

* Corresponding author at: Zhejiang University of Technology, Institute of Bioengineering, No. 18 Chaowang Road, Hangzhou 310014, Zhejiang Province, PR China. Tel.: +86 571 88320630; fax: +86 571 88320630.
E-mail address: zhengyg@zjut.edu.cn (Y.-G. Zheng).

1359-5113/$ – see front matter © 2014 Elsevier Ltd. All rights reserved.
http://dx.doi.org/10.1016/j.procbio.2014.01.003

its highly enantioselective hydrolysis of (*R,S*)-ECH were also studied.

2. Materials and methods

2.1. Strains and growth condition

E. coli JM 109 (Tiangen biotech Co., Ltd., Beijing, China) and *E. coli* BL21 (DE3) (Invitrogen, Karlsruhe, Germany) were used for gene cloning and gene expression, respectively. The *E. coli* strains were cultured in Luria-Bertani (LB) medium at 37 °C, and supplemented with the appropriate antibiotic(s) [ampicillin (100 μg/mL) or kanamycin (50 μg/mL)].

2.2. Cloning of the EH gene

Genomic DNA was extracted from strain ZJB120203 using a FastDNA® Spin Kit for Soil (MPBio, Santa Ana, CA) following the manners provided by manufacturer. To obtain the partial EH gene fragment, two degenerate primers EHF1 and EHR1 (Table 1) were designed according to the sequences of two regions (HGWPG and GHFAALE) that are highly conserved among five EHs gene (GenBank accession nos. ABF21120, AAO67343, AAF64646, CAA73331 and AFI98637). The PCR product was directly sequenced and the resulting DNA sequence was used for alignment and homology search. For cloning of the full-length EH gene, EHF2 and EHR2 primers (Table 1) were designed based on the EH gene sequence of closest homologue from strain ZJB120203. The amplified DNA fragments were cloned into the pGEM-T vector (Promega, Madison, WI, USA), and then introduced into *E. coli* JM109. The resulting plasmid was named pGEM-T-*ameh*. The successful clones were identified by direct colony PCR and subjected to plasmid isolation, then sequenced the whole length of EH gene.

2.3. Sequence analysis, homology modeling and docking

Sequence similarity searches were carried out using blastn and blastp, respectively. Sequence analyses were inferred with ExPASy [19]. A multiple alignment of EH amino acid sequences from various organisms were constructed with software package DNAMAN and the ESPript 2.2 network station [20].

The three-dimensional homology model of AmEH was generated using Build Homology Models (MODELER) in Discovery studio (DS) 2.1 (Accelrys Software, San Diego, USA) using crystal structures of EHs (PDB accession no. 4i19) as templates. The generated structures were improved by subsequent refinement of the loop conformations by assessing the compatibility of an amino acid sequence to known PDB structures using the protein Heath module in DS 2.1. The geometry of loop regions was corrected using Refine Loop/MODELER [21]. Finally, the best quality model was chosen for further calculations, molecular modeling, and docking studies by Autodock 4.0 [22].

2.4. Expression and purification of AmEH

For construction of expression vector of AmEH gene, the following pair of primers, EHF3 and EHR3 (Table 1) were synthesized, and the underlined parts were the *Nde* I and *Not* I sites. The amplified DNA fragment was double-digested with *Nde* I and *Not* I, and then ligated into pET28a expression vector treated the same restriction enzymes to construct the recombinant plasmid pET28a-AmEH. This recombinant plasmid was used for the expression of the AmEH gene in *E. coli* BL21 (DE3).

E. coli BL21 (DE3) cells harboring the pET28a-AmEH were grown at 37 °C in LB medium containing Kan (50 μg/mL) until the optical density reached 0.8 at 600 nm. Then, cells were induced by addition of 0.1 mM isopropyl-β-D-thiogalactopyranoside (IPTG) and growth was carried out at 28 °C for extra 10 h. The cells were harvested by centrifugation at 10,000 × *g* for 10 min, washed with 50 mM phosphate buffer (pH 8.0). The cell pellet was re-suspended in 50 mM phosphate buffer (pH 8.0) and disrupted by sonication. Cell debris was removed by centrifugation at 10,000 × *g* for 10 min. The soluble fraction was applied to a Nickel–nitrilotriacetic (Ni–NTA) column equilibrated with binding buffer [50 mM phosphate buffer (pH 8.0)]. After being washed with washing buffer [500 mM NaCl, 20 mM phosphate (pH 8.0) and 20 mM imidazole], the bound enzyme was eluted with elution buffer [500 mM NaCl, 20 mM phosphate (pH 8.0) and 500 mM imidazole], and then dialyzed against 50 mM phosphate buffer (pH 8.0) [23]. The collected pure enzyme was used for characterization experiments. The purity of the protein was analyzed by 12% sodium dodecyl sulfate-polyacrylamide gel electrophoresis (SDS-PAGE) under denaturing conditions as described by Laemmli [24]. The protein concentration was measured by the method of Bradford using the Bio-Rad protein assay kit with bovine serum albumin as a standard.

2.5. Enzyme assay

The standard assay was performed with racemic ECH and the recombinant EH mixed in 10 mL phosphate buffer (pH 8.0). The reaction mixture reaction was incubated at 30 °C, 150 rpm. After 10 min, 1.0 mL biotransformation sample was taken and centrifuged at 12,000 × *g* for 6 min and then 200 μL of biotransformation sample was extracted with 600 μL of ethyl acetate and centrifuged at 10,000 × *g* for 6 min. The organic layer was separated and dried with anhydrous sodium sulfate. The reaction mixture was analyzed by GC and chiral GC to determine the enzyme activity and *ee* value, respectively. The Agilent 6890N system (Agilent, Santa Clara, CA) was equipped with a capillary HP-5 column (0.35 mm × 30 m × 0.25 μL film thickness) with N_2 as carrier gas. Chiral separation was performed on a chiral capillary BGB-175 column (0.25 mm × 30 m × 0.25 μL film thickness). The initial column temperature was set at 90 °C and the inlet and detector temperatures were both 220 °C. The retention times of racemic ECH, (*S*)-ECH and (*R*)-ECH were 2.8, 4.6 and 4.8 min, respectively [25]. The *ee* was derived from the remaining epoxide of the two enantiomers

Table 1
The primers for PCR used in the study.

Primer name	Sequence	Purpose
P1	5′-AGAGTTTGATCCTGGCTCAG-3′	16S rDNA
P2	5′-AAGGAGGTGATCCAGCCGCA-3′	16S rDNA
EHF1	5′-YKSCAYGGYTGGCCMGG-3′	First partial fragment
EHR1	5′-SARYGCRGCAAAGTGTCC-3′	First partial fragment
EHF2	5′-ATGACCGCGGTGAGTCCCAC-3′	Full length amplification
EHR2	5′-TCATTGTTCATTTCCTCTCAATTG G-3′	Full length amplification
EHF3	5′-CGCCATATGACCGCGGTGAGTCC CAC-3′	Expression primer
EHR3	5′-ATTTGCGGCCGCTCATTGTTCATTTCCTCTC AATTGG-3′	Expression primer

Note: Y represents identifies C or T; K represents G or T; S represents C or G; M represents A or C; R represents A or G. Restriction sites are underlined.

[$ee(\%) = (S-R)/(S+R) \times 100$]. The extent of yield ($y$) was calculated from [$y = (A^R + A^S)/(A_0{}^R + A_0{}^S)$] before the complete consumption of epoxide, where the initial epoxide of (R) and (S) was denoted as A_0, and the remaining epoxide of (R) and (S) was as A. One unit (U) of EH activity was defined as the amount of enzyme required to convert 1 μmol ECH at 30 °C. Specific activity was defined as U/mg of enzyme.

2.6. Effects of pH and temperature on AmEH activity

The pH dependence of AmEH activity was investigated using the following buffers with concentration of 0.1 M: sodium acetate–acetic acid buffer (pH 4.0 to 7.0), boric acid-sodium borate buffer (pH 7.5 to 8.5), sodium phosphate buffer (pH 6.5 to 8.0), and glycine–sodium hydroxide buffer (pH 8.5 to 10.0). The enzyme stability at each pH was estimated by incubating the enzyme solution with 0.1 M buffers at pH 4.0–10.0 at 4 °C for 30 min. AmEH activities were measured at pH 8.0 over a temperature range of 20 to 50 °C to determine optimum temperature. For determination of the thermostability, the enzyme was pre-incubated in a water bath at different temperatures for 1 h, and then the remaining activity was assayed. All assays were performed in triplicate.

2.7. Circular dichorism (CD) measurements

CD spectra were recorded using a J-815 spectropolarimeter (Jasco Co., Tokyo, Japan). The EH were dissolved to a final concentration of 0.1 mg/mL in 20 mM sodium phosphate buffer (pH 8.0). The cell pathlength of 1.0 cm was used for the spectral range 190–350 nm. The scanning rate was 20 nm/min. Spectra manager 228 software was used for data acquisition [26,27].

2.8. Substrate specificity

Substrate specificity of AmEH was determined by measuring the enzyme activity toward various epoxides. All reactions were conducted in 0.1 M sodium phosphate buffer (pH 8.0) at 30 °C for 10 min with 50 mM substrate. The enzyme activity of AmEH toward the epoxides was determined using the following methods: Epoxides 2 and 12 were analyzed by chiral GC-14C system equipped with Chiraldex G-TA column [28,29]. Epoxides 8 to 10 were analyzed with a chiral capillary BGB-174 column. Epoxides 3 to 7 were analyzed by chiral HPLC (Daicel CHIRALPAK AS-H column) using hexane/2-propanol 4:1 v/v as mobile phase [30]. For the analysis of the conversion of epoxide 11, a β-DEX 225 column was used [31].

3. Results

3.1. Isolation and identification of strain ZJB120203

Five bacteria were isolated from the soil from coastal wetland of Yancheng city in Jiangsu province, China. Strain ZJB120203 was found to be the most suitable biocatalyst for further study, as it showed the highest specific activity on racemic ECH. It was deposited in China Center for Type Culture Collection (CCTCC, http://www.cctcc.org/), and numbered CCTCC M2012299. Strain ZJB120203 was taxonomically characterized and identified on the basis of morphological, physiological, and biochemical tests. It was found to be an aerobic, Gram-negative, rod-shaped (0.4–0.6 × 1.0–1.2 μm), motile by a single polar flagellum. Colonies cultivated on nutrient agar for 3 days were white, soft, convex and wet with smooth edges. The carbon source utilization by a standardized micromethod employing the Biolog microstation was determined (data not shown). The 16S rDNA sequence (GenBank accession no. KC589436) of strain ZJB120203 showed high similarity (99%) to the 16S rDNA sequence of *A. mediolanus*. Based on these results, the strain ZJB120203 was identified as *A. mediolanus*, and further named as *A. mediolanus* ZJB120203.

3.2. Cloning of the AmEH gene

The partial AmEH gene with length of 799 bp was amplified using *A. mediolanus* ZJB120203 genome DNA as template with the degenerate primers. Blastn searches in the GenBank databases revealed that the PCR product (799 bp) was similar to a known EH gene (GenBank accession no. JQ671543). Oligonucleotide primer EHF2 and EHR2 were derived from the amino acid sequence of closest homologue of strain. The full-length AmEH gene consisted of an ORF of 1167 bp, was amplified with the primers EHF2 and EHR2. It begins with ATG and terminating with TGA and encodes a polypeptide of 388 amino acid residue with a predicted molecular weight of 42,952 Da, and the theoretical isoelectric point was 4.8. The AmEH nucleotide sequence has been deposited in the GenBank database under accession no. JX467176.

3.3. Sequence analysis, homology modeling and docking

The amino acid sequence deduced from EH gene of *A. mediolanus* ZJB120203 was compared with those of other organisms available in the NCBI database (Fig. 1). The amino acid sequences alignment result showed that EH from *A. mediolanus* ZJB120203 showed a high homology (99%) with *Arthrobacter* sp. JBH1 (GeneBank accession no. AFI98637) [32]. But it was only 43%, 39%, 34%, 34%, 31% and 31% identical to other EHs from *Sphingomonas* sp. KC8 (ZP_09141165), *N. aromaticivorans* DSM 12444 (YP_497537), *Rhodosporidium toruloides* CBS 0349 (AAF64646), *Rhodotorula glutinis* CIMW 147 (AAF64646), *A. niger* M200 (ABF21120), and *Agrobacterium radiobacter* AD1 (CAA73331), respectively. According to protein sequences alignments (Fig. 1), this newly cloned AmEH was shown to belong to the α/β hydrolase family, the putative members of the catalytic triad were deduced to be Asp^{181}, His^{362} and Glu^{336} (highlighted in green) [33]. The two conserved tyrosine residues (Tyr^{308} and Tyr^{239}, highlighted in pink) implicated in activation of the epoxide during catalysis were also present in the EH from *A. mediolanus* ZJB120203. An HGW[O]P motif which can form an oxyanion hole can be found [9,34].

Homology modeling and molecular docking were performed to gain insights into the binding mode of the substrates and the origin of inverted enantioselectivity. The binding modes of (R)- and (S)-ECH in the active site from molecular docking are shown in Fig. 2. As shown in Fig. 2, both of (R)- and (S)-ECH form hydrogen bonds with Tyr^{308} by the epoxide oxygen. We proposed that a sufficiently small d (the distance between the Asp^{181} oxygen and the attacked epoxide carbon) value could correspond to a near-attack conformer as discussed by Bruice in other enzyme-catalyzed reaction [35], or more generally to a productive position, and that consequently, this distance should be shorter in the case of the preferred enantiomer [36]. There was a difference in d values between (R)-(3.5 Å) and (S)-ECH (3.8 Å). The Δd value is expected to be 0.3 Å, with the preferred (R)-ECH closer to the attacking Asp^{181} (Table 2). According to the near attack conformations (NACs) postulated by Bruice [37], the angle from the Asp^{181} oxygen *via* the attacked epoxide carbon to the epoxide oxygen (α_1) and the Asp^{181} oxygen *via* the attacked epoxide carbon to the other epoxide carbon (α_2) were also considered. The favored (R)-ECH has larger angles (α_1 and α_2) than the disfavored (S)-ECH (Table 2). These may be the reason that why the hydrolysis of the (R)-ECH proceeds at a much higher rate than that of the (S)-ECH.

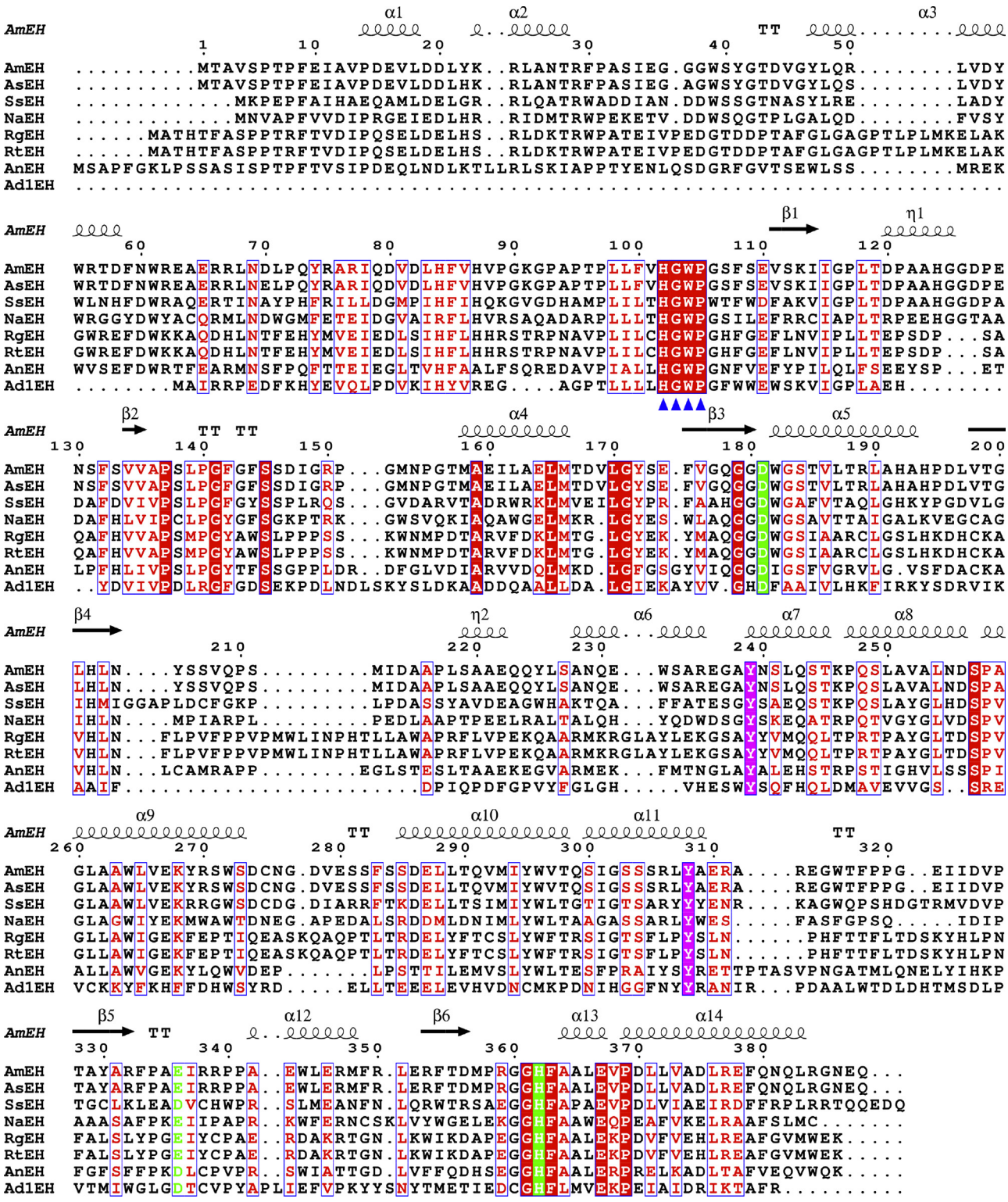

Fig. 1. Multiple alignments of amino acid sequences of EHs. The protein accession numbers are: *A. mediolanus* ZJB120203 (AmEH, this paper), *Arthrobacter* sp. JBH1 (AsEH, AFI98637), *Sphingomonas* sp. KC8 (SsEH, ZP_09141165), *N. aromaticivorans* DSM 12444 (NaEH, YP_497537), *R. glutinis* CIMW 147 (RgEH, AAF64646), *R. toruloides* CBS 0349 (RtEH, AAO67343), *A. niger* M200 (AnEH, ABF21120), and *A. radiobacter* AD1 (AD1EH, CAA73331). The amino acid residues that are conserved in all sequences are all labeled in red. The catalytic triad (Asp^{181}, His^{362} and Glu^{336}) and the two tyrosines (Tyr^{308} and Tyr^{239}) are marked in green and pink, respectively. The oxyanion hole of active site motif is marked by blue triangles. (For interpretation of the references to color in this figure legend, the reader is referred to the web version of this article.)

3.4. Expression of the AmEH gene and its purification

In order to express the AmEH gene, the recombinant expression vector pET28a-AmEH was transformed into the *E. coli* BL21 (DE3) competent cells. The recombinant cell was induced by 0.1 mM of IPTG at 28 °C for about 10 h when the OD_{600} reached the value of 0.8. Recombinant AmEH was purified from the supernatants of cell lysates by single-step affinity chromatography on a Ni–NTA

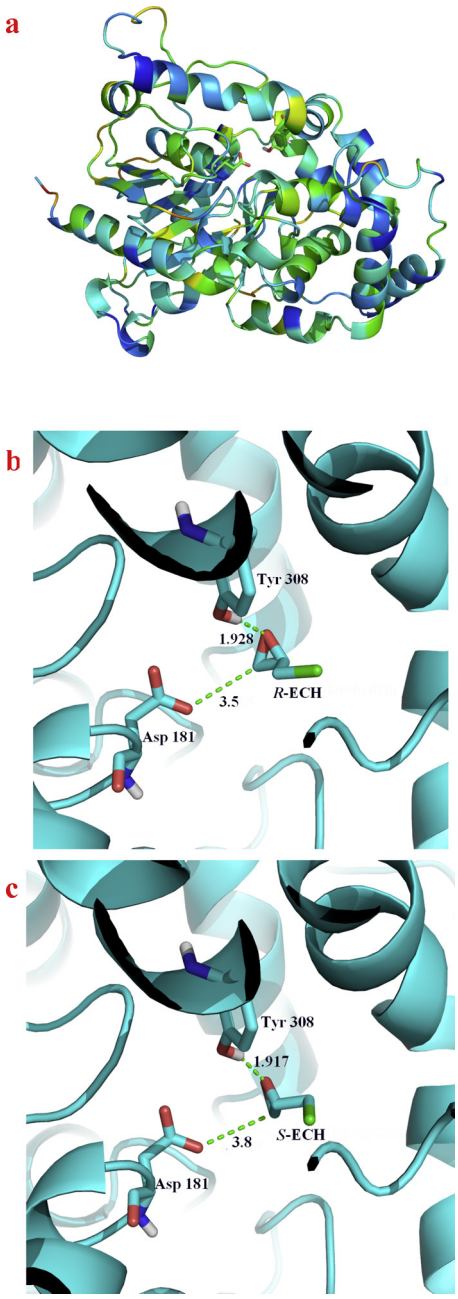

Fig. 2. Homology modeling and molecular docking. (a) Homology protein model of AmEH; (b) (*R*)-ECH docking into the active site of the enzyme; (c) (*S*)-ECH docking into the active site of the enzyme.

column. The SDS-PAGE result showed that a recombinant protein about 43 kDa (Fig. 3), which was in accordance with the predicted value, was expressed. The specific activity and amount of protein of the recombinant EH were calculated to be 24.6 U/mg and 0.11 g/L, respectively.

Table 2
Results of docking experiments.

Substrate	*d* [Å][a]	α_1 [°][b]	α_2 [°][b]
R-ECH	3.5	125.0	118.8
S-ECH	3.8	94.3	88.3

[a] *d*: the distance between the Asp^{181} oxygen and the attacked epoxide carbon.
[b] α_1: the angle from Asp^{181} oxygen *via* the attacked epoxide carbon to the epoxide oxygen; α_2: the angle Asp^{181} oxygen *via* the attacked epoxide carbon to the other epoxide carbon.

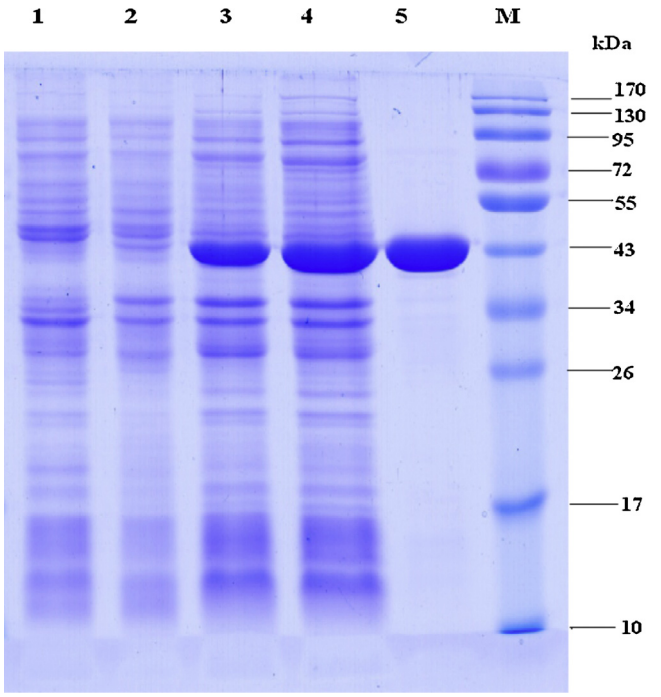

Fig. 3. SDS-PAGE analysis of expression products by *E. coli* BL21 (DE3) (pET28a-AmEH). Lane 1, *E. coli* BL21(DE3)/pET28a; lane 2, uninduced *E. coli* BL21(DE3)/pET28a-AmEH; Lane 3, *E. coli* BL21(DE3)/pET28a-AmEH induced by IPTG; Lane 4, soluble fraction of BL21(DE3)/pET28a-AmEH induced by IPTG; Lane 5, the purified AmEH; Lane M, molecular weight mark.

3.5. Biochemical characterization of the AmEH

The pH optimum was detectable in the pH range from 4.0 to 10.0. Optimum activity of AmEH toward ECH occurred at 8.0 (Fig. 4a). The AmEH showed the high activity over a broad pH range from 6.0 to 9.0. However, the enzyme exhibited little activity below pH 5.0 or above pH 9.0. The AmEH was stable at pH 6.0–9.0, it retained more than 79% residual activity after incubation at 30 °C for 30 min (Fig. 4b).

The optimum temperature of the AmEH activity was determined by incubating the purified AmEH in the reaction mixture for 10 min at temperatures from 20 to 50 °C, respectively, at pH 8.0. The purified recombinant AmEH exhibited a maximum in activity at 35 °C (Fig. 5a). Below 30 °C or above 40 °C, there was a significant decrease in the specific activity of AmEH. To determine the stability against thermal denaturation, the recombinant enzymes were pre-incubated at various temperatures (20–50 °C) for 1 h and then cooled immediately to assay the residual activity at 30 °C. The enzyme remained stable up to 35 °C (Fig. 5a), more than 80% activity after incubation at 35 °C for 1 h. CD spectroscopy is an excellent tool for rapid determination of protein secondary structures and investigation of enzyme thermostability [38]. To further investigate the enzyme thermostability, we measured the CD spectra of AmEH at different temperatures from 190 to 350 nm. The spectra showed the effect of heat incubation on the structural change of AmEH. As shown in the Fig. 5b, only little changes were observed in the CD spectra and secondary structure content of the protein at temperatures between 10 to 40 °C. But there were further changes in the CD spectra at 50, 60 and 70 °C. This result is correspond exactly with EH activity that decreased rapidly after incubation at temperatures over 40 °C.

The effects of metal ions and chemicals on the activity of the AmEH were measured by incubating the enzyme in the presence of reagents. The residual activities were assayed according to the standard method. The enzyme activity was severely inhibited by

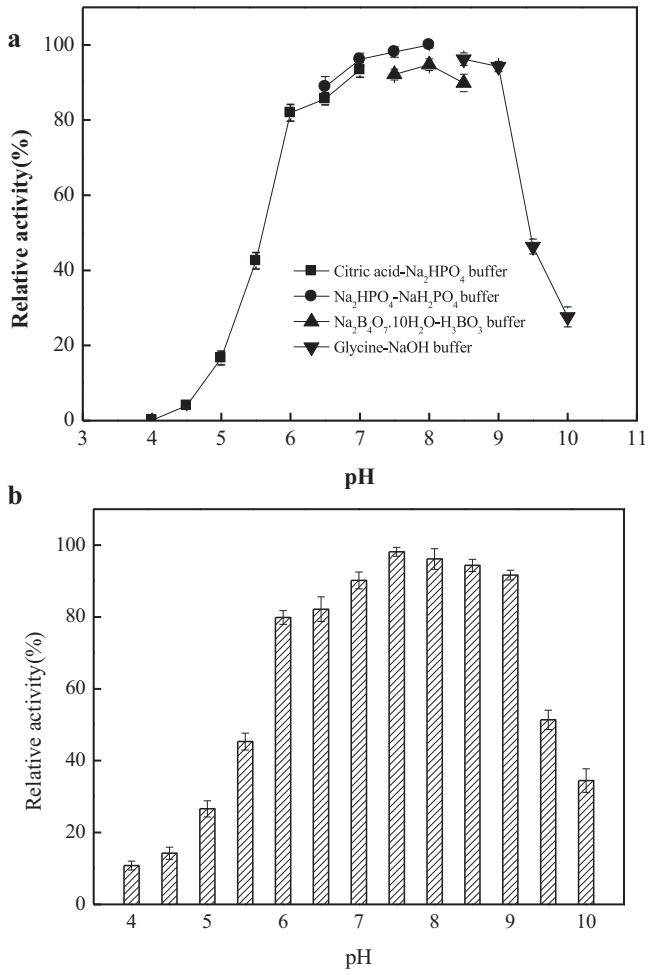

Fig. 4. Effects of pH on activity (a) and stability (b) of the purified AmEH. The activities were determined in standard conditions with 0.1 M in different buffers with pH varying from 4.0 to 10.0. The remaining activity was assayed under the enzyme assay condition after the purified recombinant enzyme had been incubated at 30 °C for 30 min in 0.1 M different buffer. The enzyme activity obtained in 0.1 M sodium phosphate buffer (pH 8.0) was taken as 100%. The results are means ± SD from three independent determinations.

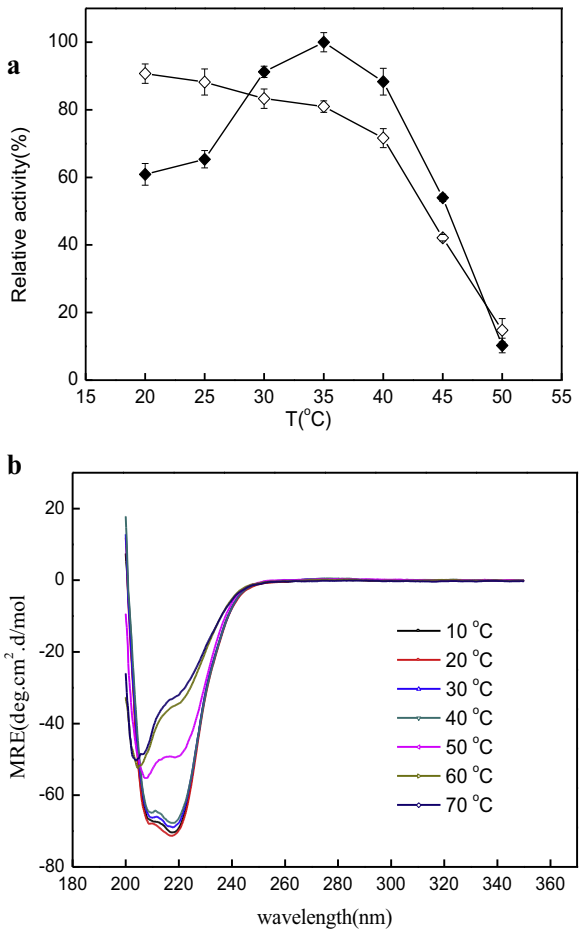

Fig. 5. Effects of temperature on the activity (♦) and stability (◊) of the purified AmEH (a). Assays were performed at various temperatures under the enzyme assay condition. The remaining activity was assayed under the enzyme assay conditions after the purified recombinant enzyme had been placed at indicated temperature for 1 h with 0.1 M sodium phosphate buffer (pH 8.0). The results are means ± SD from three independent determinations. The CD spectra of EH were collected in triplicate at wavelengths from 190 to 350 nm with a scan speed of 20 nm/min (b). (For interpretation of the references to color in this figure legend, the reader is referred to the web version of this article.)

the Hg^{2+}, Ag^{2+}, and Cu^{2+}, partially inhibited by Co^{2+}, Ni^{+}, Fe^{3+}, Ba^{2+}, Mn^{2+} and Zn^{2+}, and slightly inhibited by Mn^{2+} and Fe^{3+}. The addition of Ca^{2+}, Mg^{2+}, 2% (v/v) of Tween 80 and Triton-X100 induced the AmEH activation slightly. The metal chelator EDTA also did not inhibit the enzyme activity, indicating that this enzyme is not a metalloenzyme (Table 3).

To determine enantioselective hydrolyzing activity of the purified AmEH, hydrolysis rate of EH toward (*S*) and (*R*)-ECH were determined, and kinetic parameters were determined by nonlinear regression using a Sigma Plot program. $V_{max}{}^{R}$ and $K_m{}^{R}$ of the purified AmEH toward (*R*)-ECH were 35.62 μmol/min/mg and 56.6 mM, while $V_{max}{}^{S}$ and $K_m{}^{S}$ toward (*S*)-ECH were 7.90 μmol/min/mg and 161.4 mM respectively (Table 4), indicating that (*R*)-ECH is hydrolyzed faster than (*S*)-ECH. The enantioselectivity factor *E* was calculated as 12.9 for the hydrolysis of racemic ECH. This value is slightly higher than the *E* value of 12.2 established previously by the kinetic resolution of ECH with EH from *N. aromaticivorans* in the same aqueous phase system [16].

A number of potential substrates were tested to investigate substrate specificity of the AmEH. As shown in Table 5, the AmEH has a broad substrate specificity. Nevertheless, among these substrates there are significant differences in activity and enantioselectivity. The purified AmEH showed an enantioselective hydrolysis toward monosubstituted epoxides at C-1 position with bulky ring such as styrene oxide and benzyl glycidyl ether and with aliphatic chains such as ECH. In case of epoxides 4 to 6 which were derivative of benzyl glycidyl ether, there were marked differences in enantioselectivity with methyl position, a general trend can be found that the *ee* value increases as the methyl on the phenyl ring is shifted from the para- to the ortho-position. Thus, we further tested some other epoxides 7 to 12, however, low activity and values were observed for most of them. The activity and enantioselectivity toward glycidates-1,2-disubstitued epoxides were affected by the side chain length at C-2 position. From the results, it is concluded that the AmEH could be explored for the productions of chiral epoxides with high value, besides enantiopure (*S*)-ECH.

3.6. Enantioselective resolution of racemic ECH by purified AmEH

Biotransformation of racemic ECH by the 2 mg purified AmEH at the concentrations of 64 mM was performed under optimal reaction conditions. The time-course changes in the concentration of (*R*)- and (*S*)-ECH and the *ee* are shown in Fig. 6. The hydrolysis rate of (*R*)-ECH showed to be much faster than that of (*S*)-ECH, and (*R*)-ECH vanished completely after 35 min. The enantiopurity of the remaining (*S*)-ECH increased from 0% to >99% after 35 min. Final

Table 3
Effects of metal ions and chemical agents on AmEH activity.

Reagent	Concentration	Relative activity (%)[a]
None		100
EDTA-Na_2	5 mM	98.5 ± 1.3
$CoCl_2$	1 mM	75.8 ± 2.3
$NiCl_2$	1 mM	52.6 ± 1.7
$FeCl_3$	1 mM	87.3 ± 2.0
$BaCl_2$	1 mM	53.8 ± 0.9
$CaCl_2$	1 mM	103.7 ± 2.4
$MgCl_2$	1 mM	102.6 ± 1.2
$MnSO_4$	1 mM	89.2 ± 2.8
$ZnSO_4$	1 mM	68.5 ± 2.1
$AgNO_3$	1 mM	13.7 ± 1.8
$HgCl_2$	1 mM	0
$CuSO_4$	1 mM	19.2 ± 3.1
Triton-X100	2% (v/v)	110.3 ± 1.2
Tween 80	2% (v/v)	120.6 ± 2.5
DMSO	2% (v/v)	90.2 ± 3.7

[a] The enzyme activity was measured under the standard conditions using ECH as substrate after incubating the enzyme with different metal ions and chemical agents at 30 °C for 30 min. The activity in the absence of metal ions was recorded as 100%.

Table 4
Kinetic parameters of hydrolysis of (*S*)-and (*R*)-ECH with AmEH.

Substrate	K_m (mM)	V_{max} (μmol/min/mg)	k_{cat} (1/*s*)	k_{cat}/K_m [1/(mM s)]
(*R*)-ECH	56.6	35.62	25.74	0.453
(*S*)-ECH	161.4	7.90	5.71	0.035

yield of enantiopure (*S*)-ECH was 21.5% (theoretical yield = 50%) for racemic ECH.

4. Discussion

EHs are known to be promising biocatalysts for the preparation of chiral epoxides and vicinal diols [15,39], because of their excellent enantioselectivity on substrates. The already present application of EHs in the production of chiral epoxides is anticipated to expand as new enzymes are being isolated, cloned, and characterized.

Until now, several bacterial strains were isolated from soil samples, which can use DCP or ECH as a sole carbon source [40]. The pathway for the degradation of 1,3-dichloro-2-propanol (DCP) or ECH was found in these microorganism (Fig. S2), the dehalogenation steps are catalyzed by the haloalcohol dehalogenase, whereas the epoxide hydrolysis step is catalyzed by EH. In this paper, enrichment culture of soil samples supplemented with ECH as sole carbon source, we also added the pH indicator (bromothymol blue) in order to screen the microorganisms with the EH and halohydrin dehalogenase activity, because the ECH may be transform to 3-chloro-1,2-propanediol (MCP) by EH, and then the MCP was degraded by halohydrin dehalogenase which can cause the change of the pH. This is the first report to use this colorimetric screening and chiral GC analysis method to screen the new microorganism producing EH with enantioselectivity. Through this method, microorganisms with EH activity were rapidly found. As a result, a new strain, *A. mediolanus* ZJB120203 capable of the *R*-stereospecific epoxide hydrolysis and halohydrin dehalogenation (data not shown) was screened from soil sample.

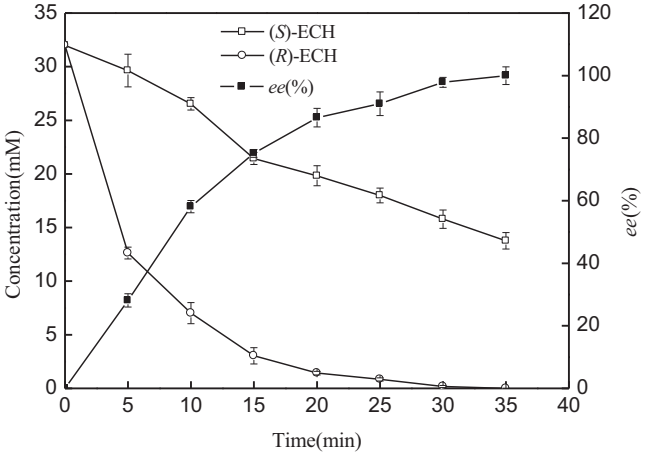

Fig. 6. Enantioselective resolution of 64 mM racemic ECH by the purified AmEH.

Further, an EH gene was isolated from strain ZJB120203. The amino acid sequences alignment showed that EH from *A. mediolanus* ZJB120203 showed a high homology (99%) with *Arthrobacter* sp. JBH1, but no information of biotransformation about the EH from the *Arthrobacter* sp. JBH1 was available**.** In addition, it was only 39% identical to EH from *N. aromaticivorans* DSM 12444 (YP_497537), which was previously used in the bioresolution of enantiopure (*S*)-ECH. Until now, about six structures of EHs belonging to α/β hydrolase family have been solved. Despite a generally low sequence similarity, EHs posses a high conservation of the catalytic triad composed of nucleophile–histidine-acid. These residues located at the interface of the main domain and the cap domain (Asp–His–Asp/Glu), while two tyrosines located in the cap domain [1]. In our case, sequence alignment and homology modeling, indicated that AmEH belongs to α/β hydrolase fold enzymes, which shares the common features in that they have critical residues to show EH activity such as the catalytic triad (Asp^{181}, His^{362} and Glu^{336}), two tyrosines (Tyr^{308} and Tyr^{239}) assisting in the ring opening and HGXP motif. It indicated that the conservativeness at the residues is the minimum requirement for EHs activity. The docking study revealed the binding mode of the substrates and the origin of inverted enantioselectivity. The Tyr^{308} make hydrogen bonds with the oxygen of the ECH, while the carboxylate oxygen of Asp^{181} is attacking one of the epoxide-ring carbons. This results in the formation of a covalent enzyme-substrate ester intermediate, which is hydrolyzed through the attack of water molecule in the second fast step of reaction. The catalytic His^{362} together with Glu^{336} function as a charge-relay pair, which is responsible for water activation. It is reported that *d* and angles value are key factors influencing the activity and enantioselectivity of EH [36]. In this study, we found that there was a big difference in angle values between (*R*)-(125.0° and 118.8°) and (*S*)-ECH (94.3° and 88.3°), which leads to the AmEH was more active on (*R*)-ECH. At the same time, the favored (*R*)-ECH shows shorter distance than the disfavored (*S*)-ECH. Regulating the *d* and angles value would improve the activity and enantioselectivity of the AmEH on (*S*)-ECH. Thus, structural changes in the binding pocket imposed by the evolutionary process are predicted to make the (*R*)-ECH to be positioned close to Asp^{181} for rapid nucleophilic attack to proceed.

The AmEH gene was successfully overexpressed in *E. coli*, and the AmEH activity was confirmed. Characterization of the recombinant AmEH showed that this enzyme has very excellent activities toward ECH and other epoxides, especially under the conditions with pH 8.0 and 35 °C. The AmEH is a potential biocatalyst for the preparation of enantiopure styrene oxide and benzyl glycidyl ether which are the important intermediate for the synthesis of pharmaceuticals and agrochemicals. The effect of selected metal ions and chemical agents >on AmEH was similar to those from other sources. Compared to the other known EHs, the racemic resolution of ECH showed that this AmEH could unusually catalyze the hydrolysis of (*R*)-ECH to produce enantiopure (*S*)-ECH [25,28,41–43]. This AmEH has been applied into resolution of 64 mM (*R*,*S*)-ECH to provide (*S*)-ECH with 21.5% yield, which is the highest yield compare to

Table 5
Comparison of the enzyme activity and enantioselectivity of AmEH toward various epoxide substrates.

Serial number	Substrates	Relative activity (%)[a]	Absolute configuration[b]	*ee* (%)
1	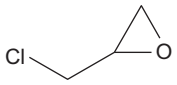 Epichlorohydrin	100	*S*	>99
2	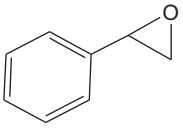 Styrene oxide	43.3	*R*	>99
3	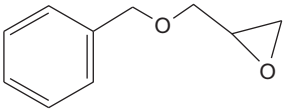 Benzyl glycidyl ether	84.9	*S*	>99
4	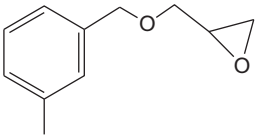 *Rac-m*-benzyl glycidyl ether	54.9	*S*	88.4
5	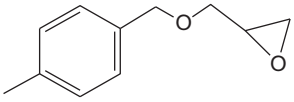 *Rac-p*-benzyl glycidyl ether	41.2	*S*	47
6	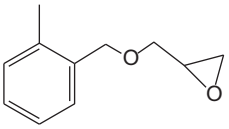 *Rac-o*-benzyl glycidyl ether	35.8	*S*	91.1
7	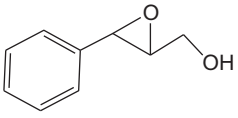 3-Phenylglcidol	51.1	(*R*,*R*)	95.7
8	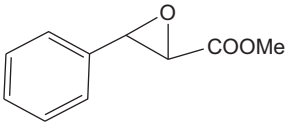 Methyl-3-phenyl glycidate	17.8	(*R*,*S*)	11.5
9	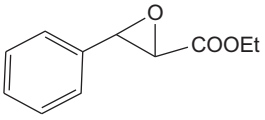 Ethyl-3-phenyl glycidate	8.6	(*R*,*S*)	9.4
10	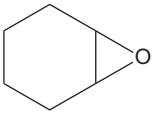 Cyclohexene oxide	15.8	–	*meso*
11	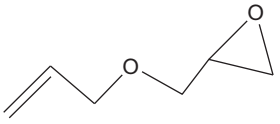 Allyl glycidyl ether	89.6	n.d.[c]	n.d.
12	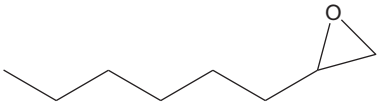 1,2-Epoxyoctane	14.5	n.d.	n.d.

[a] Value are expressed as percentage of the activity measure with ECH taken as 100%.
[b] Absolute configuration, meaning the configuration of remaining epoxide after reaction.
[c] Not determined.

previous reports [16–18]. Though the AmEH proved to have some advantages to (*S*)-ECH production, the *E*-value was indeed low, and the enzyme activity of AmEH was also required to enhance. To improve the activity and selectivity, protein engineering methods [44–48], including site-directed mutagenesis, saturation mutagenesis, error-prone polymerase chain reaction and DNA shuffling, will be applied to enhance the activity and enantioselectivity of AmEH.

In conclusion, we successfully cloned a novel EH gene from a newly isolated strain, *A. mediolanus* ZJB120203. The EH gene, with the length of 1,167 bp encoding 388 amino acids, was actively expressed in *E. coli*. The purified AmEH had a molecular mass of 43 kDa and showed its optimal activity under condition of temperature 35 °C and pH 8.0. Enantiopure (*S*)-ECH with *ee* > 99% and a yield of 21.5 were obtained from 64 mM racemates. Characteristics investigation indicated that AmEH is an attractive biocatalyst for the efficient preparation of optically active ECH.

Acknowledgments

This work was financially supported by National Natural Science Foundation of China (No. 21176224), 973 Program (No. 2011CB710806), National Major Project of Scientific Instruments Development of China (No. 2012YQ150087) and Natural Science Foundation of Zhejiang Province of China (Nos. Z4080032 and R311055).

Appendix A. Supplementary data

Supplementary data associated with this article can be found, in the online version, at doi:10.1016/j.procbio.2014.01.003.

References

[1] Arand M, Cronin A, Adamska M, Oesch F. Epoxide hydrolases: structure, function, mechanism, and assay. Method Enzymol 2005;400:569–88.
[2] Bala N, Chimni SS. Recent developments in the asymmetric hydrolytic ring opening of epoxides catalysed by microbial epoxide hydrolase. Tetrahedron: Asymmetry 2010;21:2879–98.
[3] Bellevik S, Zhang JM, Meijer J. *Brassica napus* soluble epoxide hydrolase (BNSEH1)—cloning and characterization of the recombinant enzyme expressed in *Pichia pastoris*. Eur J Biochem 2002;269:5295–302.
[4] Liu ZQ, Li Y, Ping LF, Xu YY, Cui FJ, Xue YP, Zheng YG. Isolation and identification of a novel *Rhodococcus* sp. ML-0004 producing epoxide hydrolase and optimization of enzyme production. Process Biochem 2007;42:889–94.
[5] Woo MH, Kim HS, Lee EY. Development and characterization of recombinant whole cells expressing the soluble epoxide hydrolase of *Danio rerio* and its variant for enantioselective resolution of racemic styrene oxides. J Ind Eng Chem 2012;18:384–91.
[6] Woo JH, Kang JH, Kang S, Hwang YO, Kim SJ. Cloning and characterization of an epoxide hydrolase from *Novosphingobium aromaticivorans*. Appl Microbiol Biotechnol 2009;82:873–81.
[7] Visser H, Vreugdenhil S, de Bont JAM, Verdoes JC. Cloning and characterization of an epoxide hydrolase-encoding gene from *Rhodotorula glutinis*. Appl Microbiol Biotechnol 2000;53:415–9.
[8] Kotik M, Kyslik P. Purification and characterisation of a novel enantio selective epoxide hydrolase from *Aspergillus niger* M200. BBA Gen Subj 2006;1760:245–52.
[9] Ollis DL, Cheah E, Cygler M, Dijkstra B, Frolow F, Franken SM, Harel M, Remington SJ, Silman I, Schrag J, Sussman JL, Verschueren KHG, Goldman A. The alpha/beta-hydrolase fold. Protein Eng 1992;5:197–211.
[10] Nardini M, Ridder IS, Rozeboom HJ, Kalk KH, Rink R, Janssen DB, Dijkstra BW. The X-ray structure of epoxide hydrolase from *Agrobacterium radiobacter* AD1—an enzyme to detoxify harmful epoxides. J Biol Chem 1999;274:14579–86.
[11] Archelas A, Furstoss R. Synthetic applications of epoxide hydrolases. Curr Opin Chem Biol 2001;5:112–9.
[12] Widersten M, Gurell A, Lindberg D. Structure-function relationships of epoxide hydrolases and their potential use in biocatalysis. BBA Gen Subj 2010;1800:316–26.
[13] Kotik M, Archelas A, Wohlgemuth R. Epoxide hydrolases and their application in rganic synthesis. Curr Org Chem 2012;16:451–82.
[14] Steinreiber A, Faber K. Microbial epoxide hydrolases for preparative biotransformations. Curr Opin Biotechnol 2001;12:552–8.
[15] Choi WJ, Choi CY. Production of chiral epoxides: epoxide hydrolase-catalyzed enantioselective hydrolysis. Biotechnol Bioprocess Eng 2005;10:167–79.
[16] Woo JH, Hwang YO, Kang JH, Lee HS, Kim SJ, Kang SG. Enantioselective hydrolysis of racemic epichlorohydrin using an epoxide hydrolase from *Novosphingobium aromaticivorans*. J Biosci Bioeng 2010;110:295–7.
[17] Choi WJ, Lee EY, Yoon SJ, Yang ST, Choi CY. Biocatalytic production of chiral epichlorohydrin in organic solvents. J Biosci Bioeng 1999;88:339–41.
[18] Jin HX, Hu ZC, Zheng YG. Enantioselective hydrolysis of epichlorohydrin using whole *Aspergillus niger* ZJB-09173 cells in organic solvents. J Biosci 2012;37:695–702.
[19] Gasteiger E, Gattiker A, Hoogland C, Ivanyi I, Appel RD, Bairoch A. ExPASy: the proteomics server for in-depth protein knowledge and analysis. Nucleic Acids Res 2003;31:3784–8.
[20] Gouet P, Courcelle E, Stuart DI, Metoz F. ESPript: analysis of multiple sequence alignments in PostScript. Bioinformatics 1999;15:305–8.
[21] Fiser A, Sali A. MODELLER: generation and refinement of homology-based protein structure models. Macromol Crystallogr, Part D 2003;374:461–91.
[22] Osterberg F, Morris GM, Sanner MF, Olson AJ, Goodsell DS. Automated docking to multiple target structures: incorporation of protein mobility and structural water heterogeneity in AutoDock. Proteins: Struct Funct Genet 2002;46:34–40.
[23] Liu ZQ, Dong LZ, Cheng F, Xue YP, Wang YS, Ding JN, Zheng YG, Shen YC. Gene cloning, expression, and characterization of a Nitrilase from *Alcaligenes faecalis* ZJUTB10. J Agric Food Chem 2011;59:11560–70.
[24] Laemmli UK. Cleavage of structural proteins during the assembly of the head of bacteriophage T4. Nature 1970;227:680–5.
[25] Liu ZQ, Zhang LP, Cheng F, Ruan LT, Hu ZC, Zheng YG, Shen YC. Characterization of a newly synthesized epoxide hydrolase and its application in racemic resolution of (*R,S*)-epichlorohydrin. Catal Commun 2011;16:133–9.
[26] Greenfield NJ. Using circular dichroism spectra to estimate protein secondary structure. Nat Protoc 2006;1:2876–90.
[27] Louis-Jeune C, Andrade-Navarro MA, Perez-Iratxeta C. Prediction of protein secondary structure from circular dichroism using theoretically derived spectra. Proteins 2012;80:374–81.
[28] van Loo B, Spelberg JHL, Kingma J, Sonke T, Wubbolts MG, Janssen DB. Directed evolution of epoxide hydrolase from *A. radiobacter* toward higher enantioselectivity by error-prone PCR and DNA shuffling. Chem Biol 2004;11:981–90.
[29] Elenkov MM, Hauer B, Janssen DB. Enantioselective ring opening of epoxides with cyanide catalysed by halohydrin dehalogenases: a new approach to non-racemic beta-hydroxy nitriles. Adv Synth Catal 2006;348:579–85.
[30] Wei C, Chen YY, Shen HL, Wang S, Chen L, Zhu Q. Biocatalytic resolution of benzyl glycidyl ether and its derivates by *Talaromyces flavus*: effect of phenyl ring substituents on enantioselectivity. Biotechnol Lett 2012;34:1499–503.
[31] Kotik M, Brichac J, Kyslik P. Novel microbial epoxide hydrolases for biohydrolysis of glycidyl derivatives. J Biotechnol 2005;120:364–75.
[32] Husserl J, Hughes JB, Spain JC. Key enzymes enabling the growth of *Arthrobacter* sp. strain JBH1 with nitroglycerin as the sole source of carbon and nitrogen. Appl Environ Microbiol 2012;78:3649–55.
[33] Arand M, Muller F, Mecky A, Hinz W, Urban P, Pompon D, Kellner R, Oesch F. Catalytic triad of microsomal epoxide hydrolase: replacement of Glu(404) with Asp leads to a strongly increased turnover rate. Biochem J 1999;337:37–43.
[34] van Loo B, Kingma J, Arand M, Wubbolts MG, Janssen DB. Diversity and biocatalytic potential of epoxide hydrolases identified by genome analysis. Appl Environ Microbiol 2006;72:2905–17.
[35] Bruice TC. A review at the millennium: the efficiency of enzymatic catalysis. Acc Chem Res 2002;35:139–48.
[36] Reetz MT, Bocola M, Wang LW, Sanchis J, Cronin A, Arand M, Zou JY, Archelas A, Bottalla AL, Naworyta A, Mowbray SL. Directed evolution of an enantioselective epoxide hydrolase: uncovering the source of enantioselectivity at each evolutionary stage. J Am Chem Soc 2009;131:7334–43.
[37] Schiott B, Bruice TC. Reaction mechanism of soluble epoxide hydrolase: insights from molecular dynamics simulations. J Am Chem Soc 2002;124:14558–70.
[38] Kelly SM, Price NC. The use of circular dichroism in the investigation of protein structure and function. Curr Protein Pept Sci 2000;1:349–84.
[39] Lin H, Liu JY, Wang HB, Ahmed AAQ, Wu ZL. Biocatalysis as an alternative for the production of chiral epoxides: a comparative review. J Mol Catal B: Enzym 2011;72:77–89.
[40] Nakamura T, Yu FJ, Mizunashi W, Watanabe I. Production of (*R*)-3-chloro-1,2-propanediol from prochiral 1,3-dichloro-2-propanol by *Corynebacterium* sp strain N-1074. Appl Environ Microbiol 1993;59:227–30.
[41] Kim HS, Lee JH, Park S, Lee EY. Biocatalytic preparation of chiral epichlorohydrins using recombinant *Pichia pastoris* expressing epoxide hydrolase of *Rhodotorula glutinis*. Biotechnol Bioprocess Eng 2004;9:62–4.
[42] Weijers CAGM. Enantioselective hydrolysis of aryl, alicyclic and aliphatic epoxides by *Rhodotorula glutinis*. Tetrahedron: Asymmetry 1997;8:639–47.
[43] Jin HX, Liu ZQ, Hu ZC, Zheng YG. Biosynthesis of (*R*)-epichlorohydrin at high substrate concentration by kinetic resolution of racemic epichlorohydrin with a recombinant epoxide hydrolase. Eng Life Sci 2013;13:385–92.
[44] Liu ZQ, Sun ZH, Leng Y. Directed evolution and characterization of a novel D-pantonohydrolase from *Fusarium moniliforme*. J Agric Food Chem 2006;54:5823–30.
[45] Brustad EM, Arnold FH. Optimizing non-natural protein function with directed evolution. Curr Opin Chem Biol 2011;15:201–10.
[46] Reetz MT, Prasad S, Carballeira JD, Gumulya Y, Bocola M. Iterative saturation mutagenesis accelerates laboratory evolution of enzyme stereoselectivity: rigorous comparison with traditional methods. J Am Chem Soc 2010;132:9144–52.
[47] Shivange AV, Marienhagen J, Mundhada H, Schenk A, Schwaneberg U. Advances in generating functional diversity for directed protein evolution. Curr Opin Chem Biol 2009;13:19–25.
[48] Cesarini S, Bofill C, Pastor FIJ, Reetz MT, Diaz P. A thermostable variant of *P. aeruginosa* cold-adapted LipC obtained by rational design and saturation mutagenesis. Process Biochem 2012;47:2064–71.